Nonlinear Free Surface Effects in Tank Draining at Low Gravity

C. R. EASTON*
McDonnell Douglas Astronautics Company—West Huntington Beach, Calif.

AND

IVAN CATTON†
University of California, Los Angeles, Calif.

Solutions are developed for the low-gravity draining problem, retaining all of the nonlinear terms in the free surface boundary conditions. The resultant free surface shapes are compared to published experimental data, linearized solutions, and solutions from the Marker and Cell method (finite difference solutions of the Navier-Stokes equations). Linearized analyses are shown to fail at both large and small Weber number (based on mean velocity). Domains of validity for the linearized and nonlinear analyses are found by comparison of theory and experiment. Bond number is shown to have little effect on the pull-through height for the range of Bond number of interest to orbiting spacecraft. Weber number is shown to be a better choice for correlating experimental data than Froude number.

Nomenclature

A_n = Fourier coefficients defined by Eq. (5)
B_n, B_n' = Fourier coefficients defined by Eq. (12)
Bo = Bond number, $(\rho g D^2/\sigma)$
D = tank diameter
d = drain diameter
E_n = Fourier coefficients defined by Eq. (30)
Fr = Froude number, (V_m^2/gd)
g = acceleration
H_c = surface height at the wall of pull-through
I_{nm} = matrix defined by Eq. (33)
K_n = normalization coefficient, $2/J_o^2(\lambda_n)$
P = pressure
P_s = pressure contribution due to surface tension
R = tank radius
R_d = drain radius
R_1, R_2 = principal radii of curvature of free surface
r = radius measured in units of tank radius
r_1, r_2 = principal radii of curvature of free surface measured in units of tank radius
t = time measured in units of $(\rho R^3/\sigma)^{1/2}$
$\mathbf{V}$ = velocity
V_c = characteristic velocity, $(\sigma/\rho R)^{1/2}$
V_d = drain velocity
V_m = average velocity in the tank
v = velocity measured in units of V_c
v_d = drain velocity measured in units of V_c
v_m = average velocity in the tank measured in units of V_c
We = Weber number, $\rho V_m^2 D/\sigma$
Z = vertical coordinate
z = vertical coordinate measured in units of tank radius
ξ = surface height measured in units of tank radius
$\bar{\xi}$ = mean surface height
ϕ = velocity potential measured in units of $(\sigma R/\rho)^{1/2}$
Φ = ϕ evaluated at the free surface
ψ = function defined by Eq. (28)
λ_n = roots of Eq. (6)
σ = surface tension
ρ = density

Presented as Paper 69-680 at the AIAA Second Fluid and Plasma Dynamics Conference, San Francisco, Calif., June 16–19, 1969; submitted June 27, 1969; revision received January 20, 1970. The research described in this paper was conducted under the McDonnell Douglas Astronautics Company-Western Division Independent Research and Development (IRAD) program.

* Senior Engineer/Scientist, Advance Propulsion Department, Advance Science and Technology Directorate.

† Assistant Professor of Engineering. Member AIAA.

I. Introduction

A PROBLEM of major concern in the design of orbital propellant transfer systems is vapor pull-through caused by large-amplitude deformation of the liquid surface during outflow. Pull-through results in a portion of the propellant in the tank being unusable, either for transfer to another tank or for engine supply. It is an especially serious problem in systems incorporating turbopumps, because of the potential danger of pump cavitation and destruction if gas is introduced into the system. The phenomenon is also present during satellite resupply of liquids, and may be present in certain bioastronautic systems in which liquids are transferred from tanks in a low-g environment. Certain types of maneuverable re-entry vehicles require high propellant flow rates under conditions of drag and thrust being nearly equal; in this case, pull-through could occur leaving a great deal of unusable liquid in the tank. In addition, a similar phenomenon occurs when density stratified fluids are separated by the draining of the heavier fluid from below.

The phenomenon of pull-through occurs under conditions of high liquid-outflow kinetic energy relative to the gravitational (or acceleration) potential energy. Under low-g or high-g conditions with very small tanks (low Bond number), surface tension effects may not be negligible, and surface free-energy effects must be considered. The very description of the problem indicates that it is highly nonlinear and that the surface deformation is not a small-amplitude phenomenon.

The terms "low gravity" and "low Bond number" are meant to imply that surface tension effects may not be neglected. It is not possible, at this time, to calculate draining for a Bond number so low that meniscus effects are important. This is not a limitation of the method proposed; rather it is a limitation on the available means for expressing the transient surface shape in such a manner that accurate spatial derivatives of the surface shape can be calculated. When such a means is devised, it can be readily incorporated into the method presented in this paper. This does not preclude the use of the present method for many space missions. For example, a Saturn S-IVB coasting in a near earth orbit is at a Bond number of about 200.

Analytical efforts such as those of Saad and Oliver[1] and Bhuta and Koval[2] have been somewhat unsatisfactory, because they do not maintain sufficient accuracy as pull-through is approached. Saad and Oliver completely linearized the relevant equations, whereas Bhuta and Koval kept the term that describes interaction between the surface deforma-

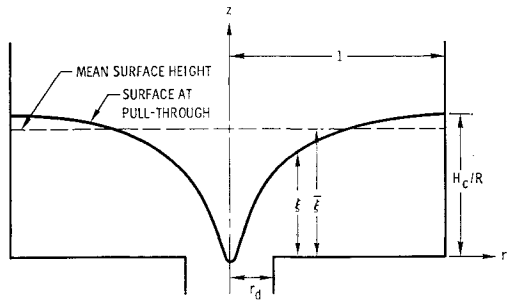

Fig. 1 Configuration variables.

tion and the average flow rate. Both analyses attempt to satisfy the free surface boundary conditions at an average free-surface height (measured from the tank bottom), which implies small deformation. The latter approximation is as important as the linearization. Lubin and Springer[3] made a momentum balance at the outlet and were able to relate the parameters of the problem, with the help of experimental data, in such a way as to yield an empirical relation between critical fluid height and outflow rate. The relationship does not allow one to determine the amount of residuals or to follow the time history of the outflow.

Experimental work has been performed in low g by Nussle, Derdul and Petrash,[4] Derdul, Grubb and Petrash,[5] and Grubb and Petrash[6] using a drop tower, and in 1-g environments with liquid and gas as well as nearly equidensity liquids by Lubin and Springer.[3] Additional extensive 1-g experiments were performed by Gluck, Gille, Zukoski, and Simpkin.[7] Most of the data on pull-through depths have been found to correlate quite well with Froude numbers for the range of conditions most suitable to the transfer of propellants in large vehicles. At low Bond numbers, the experimental data of Gluck et al.,[7] indicate that either the Bond number or Weber number must be included as another parameter. Comparison of these data with presently available linearized analyses indicates only fair agreement for the prediction of critical pull-through depths. Accurate, experimentally verified, analytical methods for the determination of residual propellant volume or pull-through time have not been achieved heretofore.

In this work, the full nonlinear dynamic and kinematic boundary conditions are used in closing the problem. The effect of surface tension is included without making the small radius of curvature approximations. The results are compared with experiment, and agreement is found to be excellent. Comparison is also made with the linearized solutions to delineate their range of applicability.

II. Governing Equations

The equations governing irrotational (inviscid) incompressible flow of a fluid with a free surface are well-known; for example, see Lamb.[8] A brief development of these equations will be presented here for completeness. The configuration variables are illustrated in Fig. 1.

Equation of Continuity

The continuity equation for an incompressible fluid is

$$\nabla \cdot \mathbf{V} = 0 \tag{1}$$

where $\mathbf{V}$ is the vector velocity. If the fluid is further constrained to be irrotational, the velocity field may be expressed as the gradient of a scalar potential ϕ, and there results

$$\nabla^2 \phi = 0 \tag{2}$$

The potential ϕ is subject to the boundary condition

$$\partial\phi/\partial n = 0 \tag{3}$$

on all solid walls where n denotes the normal to the wall. The free surface boundary conditions are discussed in a later paragraph.

For convenience, ϕ is made dimensionless such that

$$\mathbf{V} = V_c \nabla \phi \tag{4}$$

where V_c is a characteristic velocity defined by $V_c = (\sigma/\rho R)^{1/2}$ and $\nabla\phi$ is formed in coordinates dimensionless with respect to the tank radius, R.

Equation (2) is solved by separation of variables. A particular solution satisfying rotational symmetry and conditions (3), with the exception of the drain is

$$\phi_n = A_n(t) \cosh(\lambda_n z) J_o(\lambda_n r) \tag{5}$$

where λ_n is the nth positive root of

$$J_1(\lambda_n) = 0 \tag{6}$$

and A_n is an undetermined constant to be determined by satisfying the free surface boundary conditions. The boundary condition on the tank bottom is

$$V_z = V_c \left.\frac{\partial\phi}{\partial z}\right|_{z=0} = \begin{cases} 0, r > r_d \\ -V_d, r < r_d \end{cases} \tag{7}$$

where r_d is the drain radius, R_d/R, and z is the vertical coordinate measured in units of the tank radius. A second solution to Eq. (2) which also meets the cylindrical wall boundary conditions is

$$\phi_B = C_o z + \Sigma C_n e^{-\lambda_n z} J_o(\lambda_n r) \tag{8}$$

The drain velocity is then given by

$$\left.\frac{\partial\phi}{\partial z}\right|_{z=0} = C_o - \sum_n C_n \lambda_n J_o(\lambda_n r) = \begin{cases} 0, r > r_d \\ v_d, r < r_d \end{cases} \tag{9}$$

where v_d is the dimensionless drain velocity

$$v_d = V_d/V_c = -(We/2)^{1/2}/r_d^2 \tag{10}$$

and We is the Weber number based on tank diameter

$$We = \rho V_m^2 D/\sigma \tag{11}$$

The C_n are determined for $n \geq 1$ by a Fourier expansion of the right side of Eq. (9)

$$C_n = v_d K_n \int_0^{r_d} r J_0(\lambda_n r) dr \tag{12}$$

where $K_n = 2/J_o^2(\lambda_n)$. For $n = 0$,

$$C_o = v_d r_d^2 = v_m \tag{13}$$

The expansion can also be carried out for a unit value of v_d and the result written

$$C_n = C_n' v_d \tag{14}$$

where C_n' is the nth coefficient of the expansion indicated by Eq. (12) for $v_d = 1$ and is a function of r_d only.

The total potential is given by ϕ_B plus ϕ_n summed over n, hence the potential at the free surface is

$$\Phi = \sum_n A_n \cosh(\lambda_n \xi) J_o(\lambda_n r) + \Phi_B \tag{15}$$

where

$$\Phi_B = v_d C_o' \xi + v_d \sum_n C_n' e^{-\lambda_n \xi} J_o(\lambda_n r) \tag{16}$$

Equation (15) gives the value Φ that must match the specified boundary values of ϕ at the free surface.

Free Surface Boundary Conditions

There are two conditions to be satisfied on the free surface. The first is the kinematic free surface condition which requires that a particle on the free surface move with the velocity of the free surface,

$$\partial\xi/\partial t + \nabla\phi|_{z=\xi} \cdot \nabla\xi - \partial\phi/\partial z|_{z=\xi} = 0 \tag{17}$$

where time is measured in units of $(\rho R^3/\sigma)^{1/2}$. The second is the dynamical condition, the transient Bernoulli equation,

$$\partial\Phi/\partial t - \tfrac{1}{2}(\nabla\phi)^2|_{z=\xi} + P/\rho V_c^2 + (Bo/4)\,(\xi - \bar{\xi}) = 0 \quad (18)$$

where Bo is the Bond number

$$Bo = \rho g D^2/\sigma \quad (19)$$

and $\bar{\xi}$ is the mean free surface height.

The surface tension contribution to the surface forces in Eq. (18) is given by

$$\Delta P_s = \sigma(1/R_1 + 1/R_2) \quad (20)$$

where σ is the coefficient of surface tension and R_1 and R_2 are the principal radii of curvature. For cylindrical coordinates with axial symmetry, the pressure term in Eq. (18) becomes

$$\frac{P}{\rho V_c^2} = \frac{P_o}{\rho V_c^2} + \left(\frac{1}{r_1} + \frac{1}{r_2}\right) = \frac{P_o}{\rho V_c^2} + \left\{\frac{d^2\xi/dr^2}{[1 + (d\xi/dr)^2]^{3/2}} + \frac{(1/r)d\xi/dr}{[1 + (d\xi/dr)^2]^{1/2}}\right\} \quad (21)$$

where P_o, the applied pressure, is absorbed into the definition of ϕ.

Equations (17) and (18) are to be solved simultaneously to yield a boundary value of ϕ at the free surface ($z = \xi$). It should be noted that the Froude number as used by Gluck et al.,[8] is

$$Fr/d = (2v_m^2/Bo)D/d = V_m^2/gd \quad (22)$$

and the problem can be solved in terms of Fr, Bo or Fr. We as well as in terms of We and Bo.

III. Method of Solution

The basic equation, Eq. (15), has been cast into a form that meets all of the solid surface and drain boundary conditions. The free surface boundary conditions, Eqs. (17) and (18), will be met by what is essentially a variational technique. The variational technique has a complete analog in Fourier analysis, with the additional feature that the functions chosen for the expansion individually meet the boundary conditions of the problem. This enhances convergence.

Equations (17) and (18) give the time derivatives of ξ and ϕ explicitly in terms of known parameters. Hence, Eqs. (17) and (18) are written in the form

$$\partial\Phi/\partial t = F(\phi,\xi,t,r) \quad (23)$$

$$\partial\xi/\partial t = G(\phi,\xi,t,r) \quad (24)$$

where the right sides (which include all of the nonlinearities) are expressed as F and G for convenience. A finite difference technique is used to advance ϕ and ξ in time from some known set of values.

The right-hand sides of Eqs. (23) and (24) are analytic and pose no problems as far as truncation error is concerned. Lilly[9] has examined several techniques of advancing the time and concluded that the Adams-Bashforth technique was probably the best in terms of implementation and accuracy. This allows the new values of ϕ and ξ to be expressed as

$$\Phi(r,t + \delta t,z = \xi) = \Phi(r,t,z = \xi) + \delta t(\tfrac{3}{2}\partial\phi/\partial t|_t - \tfrac{1}{2}\partial\phi/\partial t|_{t-\delta t}) \quad (25)$$

$$\xi(r,t + \delta t) = \xi(r,t) + \delta t(\tfrac{3}{2}\partial\xi/\partial t|_t - \tfrac{1}{2}\partial\xi/\partial t|_{t-\delta t}) \quad (26)$$

Values of Φ and ξ are obtained at a discrete set of points spaced radially across the surface. The value of Φ obtained from Eq. (25) must be matched to the value of ϕ given by Eq. (15). This yields

$$\Phi = \sum_n A_n \cosh(\lambda_n\xi)J_o(\lambda_n r) + \Phi_B \quad (27)$$

For convenience, a new function is defined

$$\psi = \Phi - \Phi_B \quad (28)$$

and ψ is expanded in a Fourier series,

$$\psi = \sum_n E_n J_o(\lambda_n r) \quad (29)$$

which yields

$$E_n = K_n \int_0^1 \psi r J_o(\lambda_n r)dr \quad (30)$$

and on substituting into Eq. (27) and truncating to N terms yields

$$\sum_{n=1}^{N} E_n J_o(\lambda_n r) = \sum_{n=1}^{N} A_n \cosh(\lambda_n\xi)J_o(\lambda_n r) \quad (31)$$

This equation is solved for the coefficients A_n by multiplying both sides of Eq. (31) by $rJ_o(\lambda_m r)$, integrating over the radius, and taking advantage of the orthogonality of the functions. The resulting matrix equation is

$$E_m = I_{mn}A_n \quad (32)$$

where

$$I_{mn} = K_m \int_0^1 \cosh(\lambda_n\xi)J_o(\lambda_n r)rJ_o(\lambda_m r)dr \quad (33)$$

The A_n are then found by multiplying Eq. (31) by the inverse of I_{nm}. The resulting expression for A_n is

$$A_n = I_{mn}^{-1}E_m \quad (34)$$

A new expression for ϕ is now available, through Eq. (15), to be used for calculating new time derivatives of ϕ and ξ in Eqs. (23) and (24).

The above procedure is repeated for any desired length of time; e.g., until pull-through occurs. This technique of solution is relatively new to fluid mechanics, but has been applied successfully to structural mechanics for many years. As shown by Kantorovich and Krylov,[10] it is exactly equivalent to a variational statement minimizing the error of the surface fit of ϕ.

Series Convergence

When a problem is solved numerically through use of a truncated series, both the mathematical and numerical convergence of the series should be checked. The Fourier expansion of Φ [Eq. (27)] has been shown, in general, to be uniformly and absolutely convergent. The expansion of ϕ in the bulk fluid [Eq. (15)], which is matched to the free surface values of ϕ, is really a finite sequence rather than a truncated infinite series. This distinction can be made because the coefficient of any term in the expansion of ϕ depends on the number of terms taken, a result of the nonlinearity of the solution. Hence, there is no concern over mathematical convergence.

Numerical convergence implies that the number of terms is sufficient to achieve the desired accuracy and that the terms are not so large that round-off errors degrade the accuracy. The best test for numerical convergence is the sensitivity of the solution to additional terms. Figure 2 shows that the calculated critical height varies with the number of terms in the expansion of ϕ and ξ, and has virtually reached an asymptotic limit when eight terms are used in the expansion. The curve in Fig. 2 was run at a Froude number of 1.6 and a Bond number of 100. Both of these conditions are severe with respect to the number of terms required in the expansion.

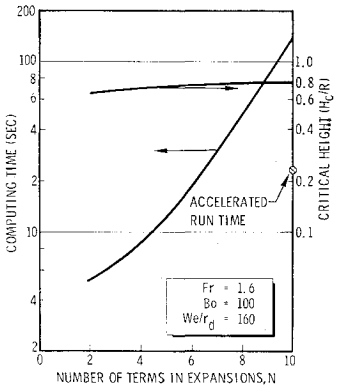

Fig. 2 Sensitivity of solution and run time to number of terms in expansions.

Superimposed on Fig. 2 is the dependence of CDC6600 computer run time on the number of terms. The asymptote shows an N^2 dependence of run time. A modification was made to the program to add terms to the expansion as they become significant. This change reduced the computer run time for a maximum of 10 terms to about 23 sec.

IV. Discussion of Results

The Bond number can be expected to play a dual role in the determination of critical or pull-through height during draining. For large Bond number, gravity will dominate surface tension as the major restoring force inhibiting pull-through. At low Bond number, meniscus effect, particularly equilibrium surface curvature, plays an important role in determining pull-through. This latter effect is beyond the scope of the present study. Meniscus effects are not admitted, even at low Bond number, because a 90° contact angle is imposed.

The Bond number enters the problem only through the free surface boundary condition [Eq. (18)]. The other dimensionless ratios appearing are the Weber number, through the drain boundary condition [Eq. (10)], and the ratio of drain diameter to tank diameter. To see what assemblage of these parameters is likely to be best for presentation of data and theoretical results, it is instructive to examine the free surface boundary conditions as linearized by Bhuta and Koval.[2] They discarded the nonlinear terms, but retained the product, $v_m\phi_z$,

$$\frac{\partial\Phi}{\partial t} = -v_m \frac{\partial\phi}{\partial z}\bigg|_{z=\xi} + \frac{1}{r}\frac{\partial}{\partial r}\left(r\frac{\partial\xi}{\partial r}\right) - \frac{Bo}{4}(\xi - \bar{\xi}) \quad (35)$$

The mean flow velocity is related to the Weber number as shown by Eq. (10). Equation (35) can be rewritten as

$$\frac{\partial\Phi}{\partial t} = \left(\frac{We}{2}\right)^{1/2}\frac{\partial\phi}{\partial z}\bigg|_{z=\xi} + \frac{1}{r}\frac{\partial}{\partial r}\left(r\frac{\partial\xi}{\partial r}\right) - \frac{Bo}{4}(\xi - \bar{\xi}) \quad (36)$$

A solution to Eq. (36) will have two parts, one has $\exp(\alpha t)$ dependence and arises from the first term on the right-hand side. The other part is found by differentiating with respect to time and substituting for $\partial\xi/\partial t$ from the linearized kinematic boundary condition.

Oscillatory solutions of the form $\exp(i\omega_n t)$,

$$\omega_n = [\lambda_n(\lambda_n^2 + Bo/4)]^{1/2} \quad (37)$$

are found for this of Eq. (36). It is easily seen that for higher modes (those that dominate pull-through) the Bond number has very little effect. For example, λ_{10}^2 is about 1000. Hence, there should be no detectable effect of Bond number at high Weber number. This result was found in both the linear and nonlinear solutions of this paper, and in the experiments of Gluck et al.,[7] and Lubin and Springer.[3]

At low Weber number, the lower-order terms in the oscillatory part of the solution may become important. For example, sudden application of the drain velocity sets up a surface oscillation which is dominated by the first mode. The result of this oscillation is that waves appear on the surface, and the centerline velocity can actually experience a reversal. There is, however, no apparent effect of this waving motion on the height of the liquid at the wall at pull-through. This result agrees with the experimental observation of Gluck et al.[8] Figure 3 shows histories of height at the centerline for different initial fill heights.

A substantially different result obtains from the linearized analysis. A marked effect of the waving motion on pull-through height is noted. Figure 4 shows that for an initial fill height of 0.45, the surface energy is sufficient to overcome the drain effect when the oscillation is at its peak amplitude. For an initial fill height of 0.35, the drain effect dominates and pull-through comes quickly.

Hence, the linearized analysis gives a completely fictitious description of the dependence of pull-through height on initial fill height at low Weber number.

The Weber number chosen for correlation to experimental data is the product of Bond number and the Froude number used by Gluck et al.[8] Figure 5 shows the range of experimental data measured by Gluck et al.,[8] and by Lubin and Springer.[3] The parameter used for correlation by Lubin and Springer is easily converted to that of Gluck with the exception of a term $r_d^{1/5}$. Superimposed on Fig. 5 are the results of the present nonlinear theory, an equivalent linearized calculation and a calculation by the Marker and Cell program.

The initial conditions posed are a flat surface impulsively started in motion at the mean velocity. The values of $\partial\phi/\partial t$ and $\partial\xi/\partial t$ at $t - \delta t$ were taken as though this motion had existed over the entire previous time step. The Bond number was varied from 10 to 1000 without a significant effect on the calculations. This does not, of course, imply that surface tension is negligible, as it appears also in the Weber number. Bond number in the experimental data ranged from 100 to 1000 and again showed no systematic effect.

The linear and nonlinear results are seen to deviate quite dramatically from one another over the entire range of Weber number considered. The error in predicting the residuals with the linearized theory will be in excess of 40% when compared with the fully nonlinear solution or with the experiment. The nonlinear theory is seen to fall within the data band over the same range of Weber number.

The Marker and Cell program (Welch et al.,[11] and Easton and Nelson[12]) solves the transient Navier–Stokes equations by finite differences. A more detailed description of the problems solved has been published by Madson et al.[13]

There are two reasons for the increasing deviation of the linear solution from the nonlinear solution at low Weber numbers. The first reason is that the potential is evaluated at the mean height and the terms associated with the drain potential have an $\exp(-\lambda z)$ type behavior. The second reason is the neglect of the $(1 + \xi_r^2)^{3/2}$ in the denominator

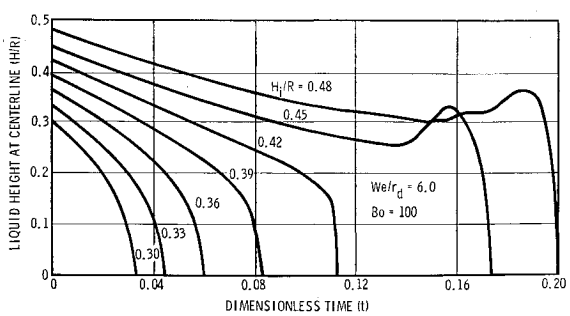

Fig. 3 Effect of fill height on centerline height history.

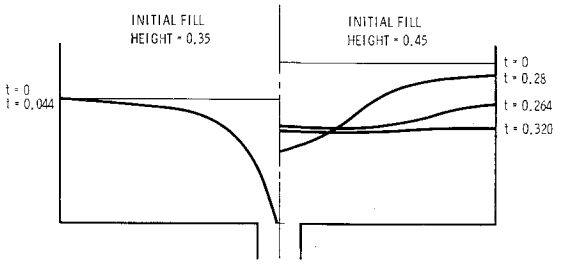

Fig. 4 Effect of initial fill height on free surface behavior, $We/r_d = 6$, $Bo = 100$.

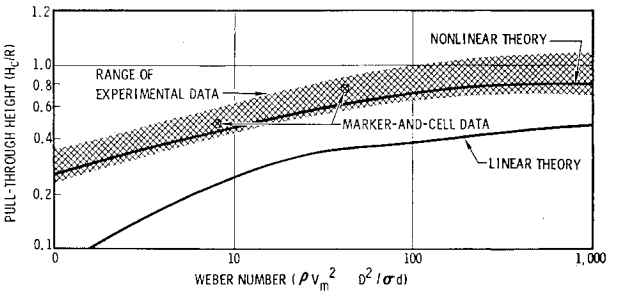

Fig. 5 Correlation of linear and nonlinear theories to experiments on pull-through height.

of the surface tension. For large suction dip (large ξ_r^2), the surface tension force is overestimated and excessively delays pull-through.

The present theory tends to fall in the lower portion of the data. The probable reason is that the Adams-Bashforth differencing method tends to damp higher order oscillations. This characteristic was shown by Lilly[9] and verified by the present analysis. The net result is that the higher order terms are not able to respond to the pull-through as rapidly as they should, thus lowering the calculated pull-through height.

The apparent reason that Gluck et al., were not able to detect a systematic effect of Bond number, even though they correlated against Froude number, is that the change of pull-through height with Weber number is less than the spread of the data for a factor of 10 change of Bond number at constant Froude number.

The zero-gravity data of Derdul et al.,[5] were not included in the above correlation, since the initial surface shape plays an important role that was not accommodated in the present theory.

V. Conclusions

The nonlinear theory of this paper has been shown to give a good correlation of the experimental data on vapor pull-through during draining, throughout the range of Weber number considered. The linear theory, run for comparison, shows a generally incorrect trend and predicts too low a critical height at all Weber numbers, with the percentage error increasing for smaller Weber number.

Weber number was shown to be a good parameter for correlating experimental data for both high and low Bond numbers because the Bond number effects are confined to initial surface shape when the parameters are arranged in this fashion. The form of the Weber number used for correlation is

$$WeD/d = \rho V_m^2 D^2/\sigma d \qquad (38)$$

The Bond number, in addition to its effect on initial surface shape, may also play an important role in the dependence of pull-through height on initial height at small Weber number.

References

[1] Saad, M. D. and Oliver, D. A., "Linearized Time-Dependent Free Surface Flow in Rectangular and Cylindrical Tanks," *Proceedings of the 1964 Heat Transfer and Fluid Mechanics Institute,* June 1964, pp. 81–99.

[2] Bhuta, P. G. and Koval, L. R., "Sloshing of a Liquid in a Draining or Filling Tank under Variable g Conditions," *Symposium on Fluid Mechanics and Heat Transfer Under Low Gravitational Conditions,* United States AFOSR and Lockheed Missiles & Space Co., 1965, pp. 10–24.

[3] Lubin, B. T. and Springer, G. S., "The Formation of a Dip on the Surface of a Liquid Draining from a Tank," *Journal of Fluid Mechanics,* Vol. 29, 1967, pp. 385–390.

[4] Nussle, R. G., Derdul, J. D., and Petrash, D. A., "Photographic Study of Propellant Weightlessness," TN D-2572, 1965, NASA.

[5] Derdul, J. D., Grubb, L. S., and Petrash, D. A., "Experimental Investigation of Liquid Outflow from Cylindrical Tanks During Weightlessness," TN D-3746, 1966, NASA.

[6] Grubb, L. S. and Petrash, D. A., "Experimental Investigation of Interfacial Behavior Following Termination of Outflow in Weightlessness," TN D-3897, 1967, NASA.

[7] Gluck, D. F. et al., "Distortion of the Liquid Surface During Tank Discharge," *Journal of Spacecraft and Rockets,* Vol. 3, No. 11, Nov. 1966, pp. 1691–1692.

[8] Lamb, H., *Hydrodynamics,* 6th ed., Dover, New York, 1945.

[9] Lilly, D. K., "On the Computational Stability of Numerical Solutions of Time Dependent Nonlinear Geophysical Fluid Dynamics Problems," *Monthly Weather Review* Vol. 93, No. 11, 1965, pp. 11–26.

[10] Kantorovich, L. V. and Krylov, V. I., "Approximate Methods of Higher Analysis," Noordhoof Ltd., Groningen, the Netherlands, 1958.

[11] Welch, J. E. et al., "The MAC Method," Rept. LA-3425, 1965, Los Alamos Scientific Lab., Los Alamos, N. Mex.

[12] Easton, C. R. and Nelson, J. B., "The MDAC-WD Version of the Marker-and-Cell Program," Rept. MDAC-62426, 1969, McDonnell Douglas Astronautics Corp.

[13] Madson, R. A., et al., "Numerical Analysis of Low-g Propellant Flow Problems," *Journal of Spacecraft and Rockets,* Vol. 7, No. 1, Jan. 1970, pp. 89–91.